

Direct evidence of light confinement and emission enhancement in active silicon-on-insulator slot waveguides

M. Galli,^{a)} D. Gerace,^{b)} A. Politi, M. Liscidini, M. Patrini, and L. C. Andreani

Dipartimento di Fisica "A. Volta," Università degli Studi di Pavia, via Bassi 6, 27100 Pavia, Italy

A. Canino, M. Miritello, R. Lo Savio, A. Irrera, and F. Priolo

MATIS CNR-INFM, Via S. Sofia 64, 95123 Catania, Italy and Dipartimento di Fisica e Astronomia, Università di Catania, Via S. Sofia 64, 95123 Catania, Italy

(Received 2 August 2006; accepted 31 October 2006; published online 14 December 2006)

The authors experimentally demonstrate strong light confinement and enhancement of emission at $1.54 \mu\text{m}$ in planar silicon-on-insulator waveguides containing a thin layer (slot) of SiO_2 with Er^{3+} doped Si nanoclusters. Angle-resolved attenuated total reflectance is used to excite the slab guided modes, giving a direct evidence of the strong confinement of the electric field in the low-index active material for the fundamental transverse-magnetic mode. By measuring the guided photoluminescence from the cleaved-edge of the sample, the authors observe a more than fivefold enhancement of emission for the transverse-magnetic mode over the transverse-electric one. These results show that Si-based slot waveguides could be important as starting templates for the realization of Si-compatible active optical devices. © 2006 American Institute of Physics.

[DOI: 10.1063/1.2404936]

The ability to guide and confine light in nanometer-size spatial regions is essential for the development of highly integrated multifunctional optoelectronic devices. In this respect, silicon-on-insulator (SOI) optical waveguides have been recognized as very promising systems due to their high index contrast, which allows to guide, bend, and confine light very efficiently by means of total internal reflection while keeping low propagation losses and full compatibility with complementary metal oxide semiconductor technology.^{1,2} More recently, a novel structure for guiding and confining light in nanometer-size low-index regions has been proposed and realized.^{3,4} This system, called *slot waveguide*, consists in a very thin slot of a low-index material (few tens of nanometer thick) embedded between two high-index material regions, which form the core of an optical waveguide. In this configuration the waveguiding/confining mechanism exploits the discontinuity of the normal component of the electric field which develops at the high-index-contrast interfaces of the slot. The ability of slot waveguides to strongly concentrate the electromagnetic field within very narrow spatial regions ($\ll \lambda$) makes them attractive systems for enhancing radiation-matter interaction. Very recently, several optoelectronic devices incorporating an optically active material in a slot waveguide geometry have been proposed theoretically.⁵

In this letter we report on the realization and optical characterization of planar SOI waveguides containing a slot of Er^{3+} doped Si nanoclusters (nc) in a low-index SiO_2 matrix as an active medium. In particular, the use of both Er^{3+} doped SiO_2 and Si-nc as an active material is very promising. In fact, high emission efficiencies due to the energy transfer between Si-nc and Er^{3+} ions⁶ together with optical gain⁷ and electrical pumping⁸ have been observed. We demonstrate the strong confinement properties of these slot

waveguides, which lead to enhanced light emission within the thin active layer. Results presented here show that this kind of structures may be usefully employed as building blocks for active photonic devices operating at telecommunication wavelengths.

Planar slot waveguides were fabricated by depositing a core on top of a $1.9\text{-}\mu\text{m}$ -thick SiO_2 clad layer thermally grown on a Si substrate. A schematic of the sample cross section is shown in Fig. 1(a). A thin layer (slot) of low-refractive-index active material of thickness d_s is placed in

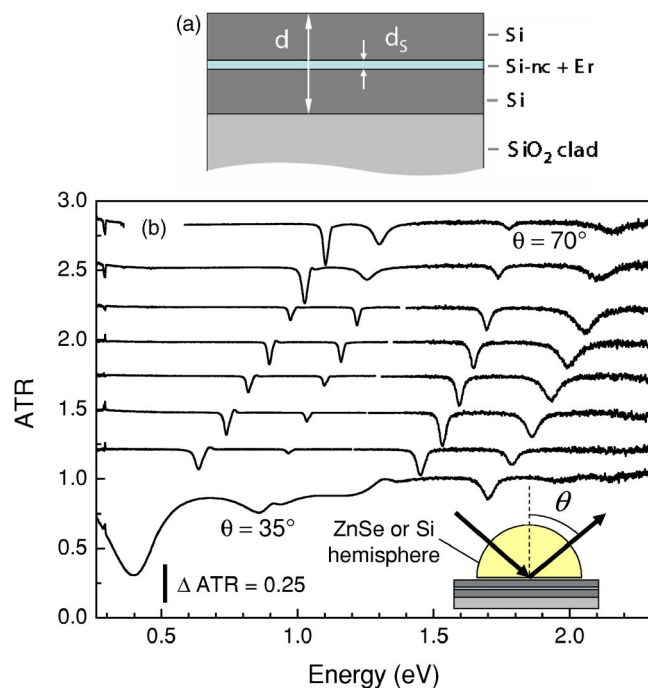


FIG. 1. (a) Schematic of the planar slot waveguide. (b) Experimental angle-resolved ATR spectra for sample S2. The angle of incidence θ increases in steps of 5° . The curves are vertically shifted for clarity. The experimental geometry used in the ATR measurements is shown in the inset.

^{a)}Electronic mail: galli@fisicavolta.unipv.it

^{b)}Also at Institute of Quantum Electronics, ETH Zurich, CH-8093 Zurich, Switzerland.

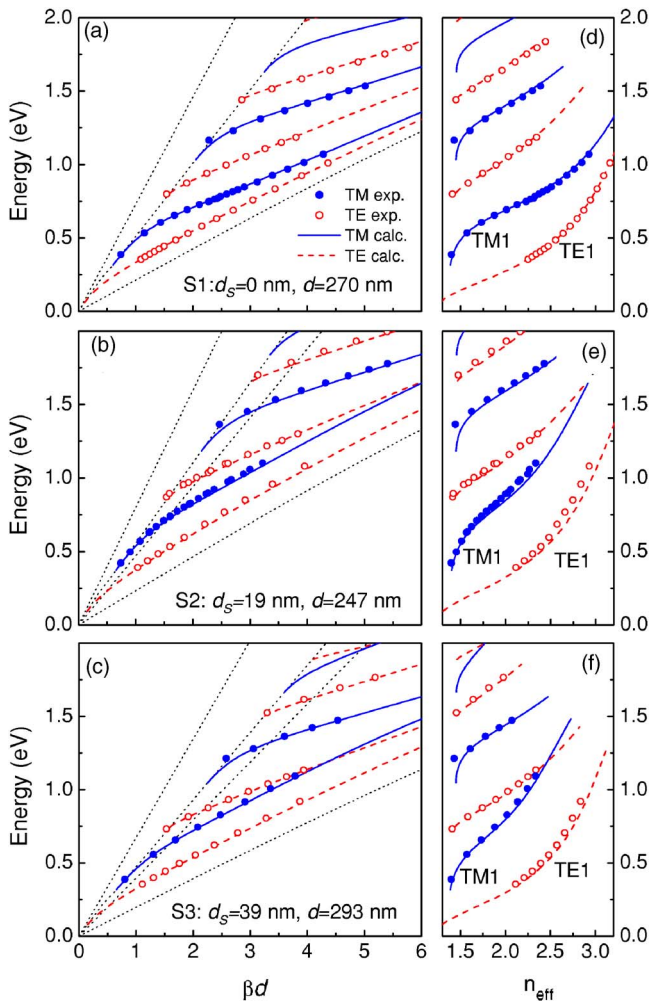


FIG. 2. Left panels: measured dispersion of TM (full circles) and TE (open circles) waveguide modes as derived from ATR spectra, compared to calculated dispersion (solid and dashed lines, respectively) for samples S1, S2, and S3. Right panels: mode effective indices as derived from ATR measurements, compared to calculated ones.

the center of the waveguide core of total thickness d . The core, made of a sequence of $\text{Si}/\text{Si-nc:Er}/\text{SiO}_2/\text{Si}$ layers, was realized by radio frequency confocal magnetron sputtering. The thin slot layer consists of an Er-doped substoichiometric silicon oxide which was deposited by the cosputtering of three targets, Si, SiO_2 , and Er_2O_3 . The Si concentration was 37 at. % and the Er content was $3.8 \times 10^{20} \text{ cm}^{-3}$, as verified by Rutherford backscattering spectrometry. After deposition the films were annealed at 900°C for 1 h in a nitrogen atmosphere in order to induce the separation of the Si and SiO_2 phases, the formation of Si nc, and the activation of the Er^{3+} ions. Si-nc have typical dimensions of a few nanometers and are densely distributed in the SiO_2 matrix, yielding an optically homogeneous slot layer with average refractive index $n=1.7$. Three different waveguides were grown with the following parameters: S1 with $d_s=0$ nm, $d=270$ nm (reference SOI waveguide); S2 with $d_s=19$ nm, $d=247$ nm; and S3 with $d_s=39$ nm, $d=293$ nm.

To excite the guided modes of the slot waveguides, we performed angle-resolved attenuated total reflectance (ATR) measurements in the spectral range of 0.3–2.4 eV, at a resolution of 0.5 meV, by means of a microreflectometer coupled to a Fourier-transform spectrometer (Bruker IFS66s). The

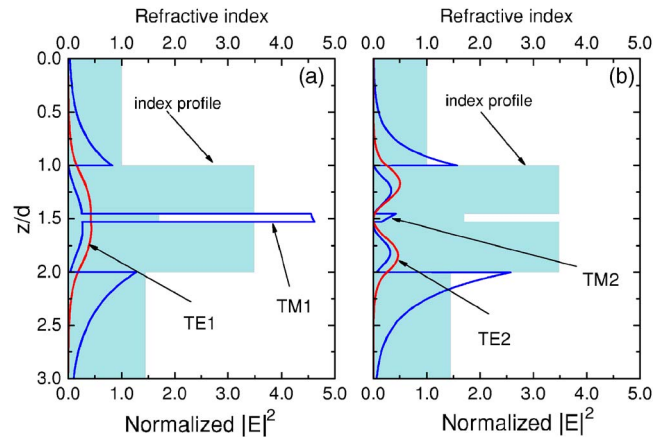


FIG. 3. Plot of calculated normalized field intensity in the slot waveguide S1 for (a) TE1 and TM1 modes at 0.8 eV and (b) TE2 and TM2 modes at 1.5 eV. Waveguide refractive index profile is also shown.

angle of incidence θ is varied in the range of 30° – 70° with an angular resolution of 0.5° . ATR spectra were measured in the Otto configuration⁹ with a high-index hemisphere (ZnSe or Si) kept at a small distance of ~ 100 – 200 nm from the sample surface by means of three piezoelectric actuators.¹⁰ This way, the guided modes of the structure can be efficiently excited through evanescent coupling by optimizing the separation distance between the hemisphere and the sample.

Angle-resolved ATR spectra were measured for all the three waveguides. Figure 1(b) shows the spectra obtained for sample S2. Deep and well defined “absorptionlike” resonances are clearly visible and mark the excitation of the guided modes of the slab. By increasing the angle of incidence θ , the resonances undergo a blueshift in energy as a consequence of the increased parallel wave vector component of the exciting radiation $\beta=(\omega/c)n_{\text{prism}}\sin\theta$. Notice that the combined use of ZnSe and Si as ATR materials allows the operation over a broad energy–wave-vector range, yielding the excitation of the fundamental as well as the high-order guided modes for both polarizations.

To demonstrate the light confinement properties of the low-index slot layer, we extract the dispersion of the guided modes from ATR spectra. Figure 2 (left panels) shows the dispersion curves for both the reference waveguide S1 and the two slot waveguides S2 and S3. The energies of ATR resonances are plotted versus the normalized wave vector βd for each sample. Experimental data are compared to the dispersion of guided modes calculated by an exact solution of Helmholtz equation with transfer-matrix method.^{11,12} Guided modes are separated according to the field orientation with respect to the plane of incidence, i.e., TE modes (electric field perpendicular to the plane) and TM modes (magnetic field perpendicular to the plane). The effect caused by the thin low-index slot is immediately evident by looking at the dispersion curves. While the dispersion of TE modes remains almost unchanged for all samples, a strong modification in the dispersion of the first TM mode (TM1) is observed for samples S2 and S3 with respect to the reference waveguide S1. As a result, the TM1 mode is substantially raised in energy relatively to the TE1 mode. This effect is even more pronounced for the thicker slot sample S3, where the TM1 mode eventually crosses the TE2 mode for $\beta d \sim 4$.

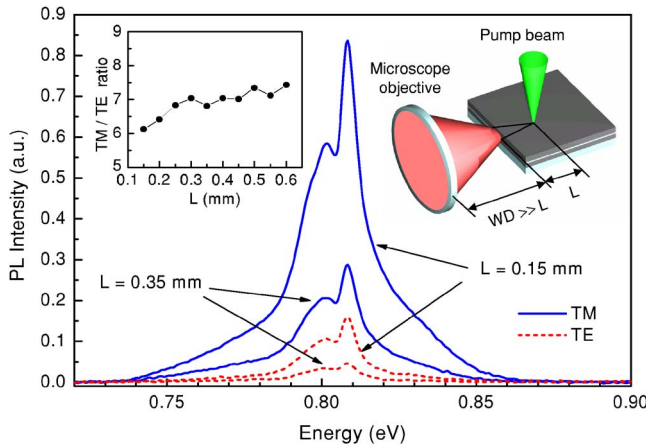


FIG. 4. Room-temperature guided PL spectra of sample S2 for TE and TM polarizations. A schematic of the experimental geometry is also shown. Inset: spectrally integrated TM/TE ratio as a function of the distance L .

From the dispersion of the guided modes, we evaluate the modal effective index as $n_{\text{eff}} = \beta c / \omega$, as reported in Fig. 2 (right panels). This is an important parameter because it reflects the degree of confinement for each mode. It is clearly seen that the slot of low-index material strongly reduces the effective index of the TM1 mode. For instance, we observe that n_{eff} at 0.8 eV for the TM1 mode decreases from 2.35 to 1.83 when going from the reference sample S1 to the slot waveguide S2. This demonstrates that for this particular mode the field intensity is strongly concentrated in the slot. It is interesting to notice that confinement effect does not occur for the TM2 mode, i.e., the TM2 effective index is not altered by the presence of the slot. This can be understood by looking at the field distributions. In Figs. 3(a) and 3(b) the normalized field intensities are plotted for the first and second order modes in the case of sample S2. The refractive index profile of the waveguide is also reported. Due to the discontinuity of the normal component of the electric field at the slot interfaces, the TM1 mode is strongly localized in the low-index slot, while the TE1 mode is only slightly affected. On the other hand, the TM2 mode is close to be an odd one (the E_z component would have a node for a symmetric slab) and is almost unaffected by the slot, as observed in the experiments.

The strong field confinement observed for the TM1 mode leads to an increase of the density of electromagnetic states. Therefore, a modification of emission from the active material located inside the slot should also be expected. We measured the guided photoluminescence (PL) spectra around $1.54 \mu\text{m}$ by exciting the slot waveguide from the top and collecting the light emitted in the guided modes from the cleaved-edge of the sample (see scheme in Fig. 4). A 532 nm Nd:YAG (yttrium aluminum garnet) laser focused to a $50 \mu\text{m}$ spot at a variable distance L from the waveguide edge has been used for the excitation. A high numerical aperture ($\text{NA}=0.4$) long working distance ($\text{WD}=20 \text{ mm}$) microscope objective focused on the facet of the sample is used for collection and is coupled to the Bruker spectrometer. The experimental configuration is essentially the shifting excitation spot scheme.^{13,14} In Fig. 4 we show selected polarization-resolved PL spectra obtained for two different values of L .

Spontaneous emission for TM polarization at the peak results to be more than five times higher than for TE polarization, thus pointing to a much stronger field confinement in the slot layer for the TM mode.

The PL intensities are found to decrease exponentially for increasing L and allow to estimate the propagation losses, which are comparable for TE and TM polarizations and close to 55 and 50 cm^{-1} , respectively. These relatively high values follow from the use of slabs with polycrystalline silicon. Notice that the exponential decay of PL for increasing L also indicates that the measurements are free from coupling artifacts.^{13,14} In order to investigate the role of polarization-dependent losses on the observed PL enhancement, we plot the ratio between TM- and TE-polarized PL, integrated over the emission range, as a function of distance L (inset of Fig. 4). The ratio TM/TE increases slowly for increasing L as a result of slightly higher TE losses, but its value remains always higher than 6. This indicates that the observed PL enhancement is only weakly affected by waveguide losses, which are mainly caused by the overlap of the modes with polycrystalline silicon. The polarization dependence of the emission intensity follows instead from the different field confinement of TE1 and TM1 modes in the active layer and constitutes additional evidence, beyond that given by ATR measurements, of the confinement properties of these slot waveguides.

In conclusion, active SOI slot waveguides have been fabricated and characterized by ATR and guided PL spectroscopy. Strong light confinement properties as well as enhanced emission into the fundamental TM mode have been demonstrated. These results are promising for the realization of efficient active Si-based optoelectronic devices such as electrically driven optical amplifiers.

The authors are indebted to F. Iacona and G. Franzò for collaboration with sample fabrication and to D. Bajoni for participating in the early stages of this work. The authors acknowledge support by MIUR through FIRB project “Miniaturized electronic and photonic systems.”

¹Y. A. Vlasov and S. J. McNab, Opt. Express **12**, 1622 (2004).

²K. K. Lee, D. R. Lim, L. C. Kimerling, J. Shin, and F. Cerrina, Opt. Lett. **26**, 1888 (2001).

³V. R. Almeida, Q. Xu, C. A. Barrios, and M. Lipson, Opt. Lett. **29**, 1209 (2004).

⁴Q. Xu, V. R. Almeida, R. R. Panepucci, and M. Lipson, Opt. Lett. **29**, 1626 (2004).

⁵C. A. Barrios and Michal Lipson, Opt. Express **13**, 10092 (2005).

⁶F. Priolo, G. Franzò, D. Pacifici, V. Vinciguerra, F. Iacona, and A. Irrera, J. Appl. Phys. **89**, 264 (2001).

⁷H. S. Han, S. Y. Seo, and J. H. Shin, Appl. Phys. Lett. **79**, 4568 (2001).

⁸F. Iacona, D. Pacifici, A. Irrera, M. Miritello, G. Franzò, F. Priolo, D. Sanfilippo, G. Di Stefano, and P. G. Fallica, Appl. Phys. Lett. **81**, 3242 (2002).

⁹A. Otto, Z. Phys. **216**, 398 (1968).

¹⁰M. Galli, M. Belotti, D. Bajoni, M. Patrini, G. Guizzetti, D. Gerace, M. Agio, L. C. Andreani, and Y. Chen, Phys. Rev. B **70**, 081307 (2004).

¹¹P. Yeh and A. Yariv, *Optical Waves in Crystals* (Wiley, New York, 1984).

¹²Dispersion of the refractive indices is taken into account in order to get an agreement in the whole spectral range.

¹³J. Valenta, I. Pelant, and J. Linros, Appl. Phys. Lett. **81**, 1396 (2002).

¹⁴L. Dal Negro, P. Bettotti, M. Cazzanelli, D. Pacifici, and L. Pavesi, Opt. Commun. **229**, 337 (2004).